Solar Physics
DOI: 10.1007/•••••-•••-•••-••••-•

Automation of tracking various sunspot group entities and demonstrating its usage on the flaring NOAA AR 11429

L. Győri

Abstract A method based on set and graph operations was developed to find and track related entities of sunspot groups on a series of consecutive solar images. Of course, if we can track entities of a sunspot group, we can also track various properties (*e.g.*, position, area, magnetic field, and intensity) associated with them. A new higher-level sunspot-group entity belonging to the whole image series, a family, was introduced to cope with the mergings and separations of various sunspot group entities.
To demonstrate the usefulness of the method it was applied to NOAA AR 11429 using *Solar Dynamics Observatory/Helioseismic and Magnetic Imager* (SDO/HMI) images. This large sunspot group produced several X, M, and C class flares, among others an X5.4 class one on 2012 March 7. Abrupt transient and permanent variations in the mean line-of-sight (LOS) magnetic field of the large umbra families were found during the X5.4 flare. Two small umbra families immediately next to the polarity inversion line (PIL) and facing each other at opposite sides of the PIL exhibited abrupt step changes in their mean LOS magnetic field during the X5.4 flare. The one with positive polarity decreased and the other with negative polarity increased. Some of the large umbra families also showed abrupt decrease in their darkness during the flare. We conjecture that an umbra family being a part of a long, narrow magnetic field strip pushing in an opposite magnetic polarity penumbral domain might be one of the triggering causes of several flares. Flare-related changes were observed at every spatial scale of the studied sunspot group. Two of the large opposite polarity-umbra families underwent shearing and converging motions. The break and the turning points of the motion curves of these families were related to flares. Some of the flares coincided with abrupt changes in the motion curves.

Keywords: sunspot tracking – sunspot – solar flare

Heliophysical Observatory, Research Center for Astronomy and Earth Sciences, Hungarian Academy of Sciences, Gyula Observing Station, 5701 Gyula, P.O. Box 93, Hungary email: lajos.gyori49@gmail.com

1. Introduction

Sunspot groups are found in solar active regions (ARs). The groups can be broken down into sunspots and pores: spots have filamentary penumbral structure, pores have not. A sunspot can be separated into penumbra and umbra(e).

Most solar flares are associated with sunspot groups and studying how flares manifest in different properties of various sunspot group entities may help in understanding and forecasting flares.

A number of papers were devoted to flare-related changes in various properties in different parts of solar active regions. Changes in the magnetic field were discovered (*e.g.*, Kosovichev and Zharkova, 2001; Wang *et al.*, 2002; Wang *et al.*, 2005; Petrie and Sudol, 2010; Liu *et al.*, 2012; Wang *et al.*, 2012a; Gosain, 2012; Murray, Bloomfield, and Gallagher, 2012; Petrie, 2013). Flare associated intensity changes were reported by several authors (*e.g.*, Liu *et al.*, 2005; Deng *et al.*, 2005; Wang and Liu, 2011; Wang, Deng, and Liu, 2012). Flare related motions were also revealed in ARs (*e.g.*, Dezső *et al.*, 1980; Schmieder *et al.*, 1994; Raman, Ramesh, and Selvendran, 2003; Brown *et al.*, 2003; Yang *et al.*, 2004; Zhang, Li, and Song, 2007; Tan *et al.*, 2009; Gosain, Venkatakrishnan, and Tiwari, 2009; Vemareddy, Ambastha, and Maurya, 2012).

These investigations provided evidence that several properties of an AR show transient-like or stepwise-like behavior during a flare. Among other things it was also found that the magnetic field becomes more horizontal after flares as suggested by Hudson, Fisher, and Welsh (2008) and Fisher *et al.* (2012)

In this paper we study the evolution of various sunspot group entities exhibiting flare-related changes. To this end, we develop a method to track these entities in images taken with high cadence.

2. Tracking sunspot group entities

When we investigate the time evolution of a sunspot group in a series of solar images, a need for tracking various entities (pore, spot, umbra, and penumbra) emerges. But, over time these features change and evolve. For example, a sunspot or an umbra can split into parts or more of them can merge into one. These processes create new entities, but they are not brand-new ones, these entities are related to the old ones. Thus, it is useful to introduce new types of entities that have broader sense, they are bound to a series of solar images, not only to individual images.

If the entities neither have significant motion in heliographic coordinates nor significant change in area between images, then set operations lend themselves to find relations among entities (considered as pixel sets) in two consecutive images. Such an image sequence is provided, for example, by the *Solar Dynamic Observatory* imagery with cadence of 45 s.

Overlap of the objects between two images were used to identify an object in one image with an object in the next image in several papers (*e.g.*, Strous *et al.*, 1996; Hagenaar *et al.*, 1999; Welsch and Longcope, 2003)

However before using set operations we should transform the pixels of image I_1 into the pixels of image I_2. It can be achieved by transforming the pixels of

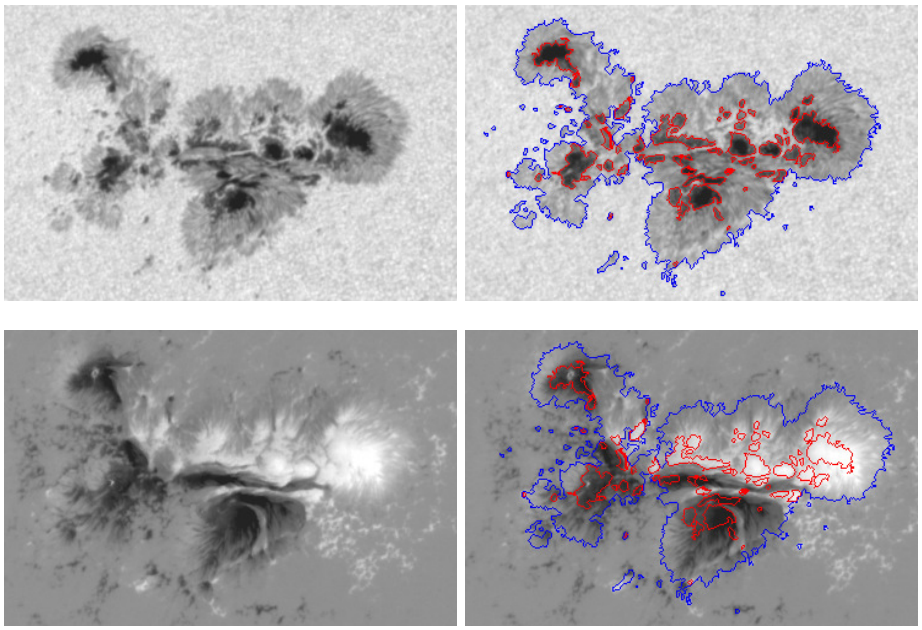

Figure 1. White light images (top row) and magnetograms (bottom row) of NOAA AR 11429 taken on 2012 March 7 at 00:23:44 UT. The blue and red pixels in the images of the second column are boundary pixels of the penumbrae and the umbrae, respectively. Note that the spot boundaries determined for the intensity image are superimposed on the magnetogram. As for how penumbra and umbra boundaries are determined, see Győri (1998).

image I_2 into heliographic coordinates and then transforming these heliographic coordinates into the pixels of image I_2. By defining the mapping between images this way, images with different scales and orientations can be used for determining entity relations.

We define two relations between entities in two consecutive images: a broader one (R_b, broad) and a narrower one (R_s, sameness). The first one describes the relation of the part and the whole. If an entity splits into several parts then this entity is considered as related to whichever part and vice versa. Moreover, if several entities merge into one entity then the newly created entity is considered as related to whichever of the former entities and vice versa. The second one describes the sameness of an entity in two consecutive images.

2.1. Sameness relation

In the first case, we regard two entities of the same class in two images as the same one. We do not require that the two entities have intersection only with each other. Both of them can have intersections with other entities in the other image, but the sum of these intersections should be small relative to the their common intersection. The reasoning for this is that during the time elapsed between the exposures of the two images the entities of the second image may move on the

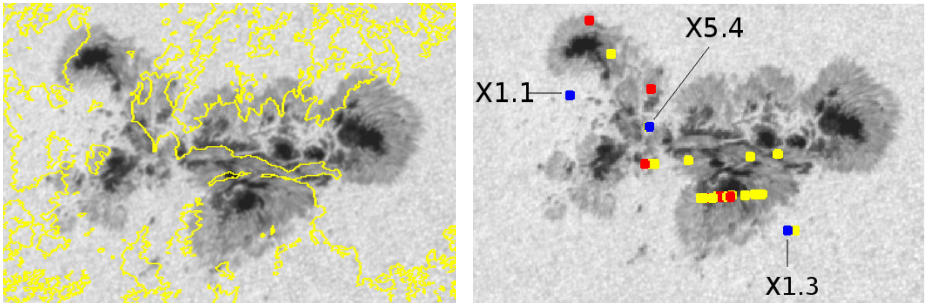

Figure 2. Left panel: Polarization inversion lines superimposed on the image (yellow lines). Right panel: flare positions superimposed on the image, blue, red, and yellow patches designate X, M, and C class flares, respectively. Flare positions superimposed on this image are those ones that the flares had in heliographic coordinates (with the precision of half a heliographic degree) at the time of their occurrences. However, for most of the flares, there are time difference between their occurrences and the time when this image was taken. During this time interval, the structure of the sunspot group might have evolved, and, moreover, the sunspot group entities might have some proper motions too. As a consequence of the inaccuracy in the flare positions and the structural and the motional changes, the flare positions, *e.g.,* relative to the umbrae might be different than suggested by this image. The image was acquired at the peak time (2012 March 7 00:23:44 UT) of the X5.4 flare.

solar surface and their sizes may also change causing overlaps that do not mean real relations. However we require that the common intersection should be large enough relative to whichever size of the two entities. The rationale for this is that when small fragments split off from an entity the newly created main part (if large enough) is considered as the same entity and, similarly, if several small entities merge into a larger one we regard the larger one (if it is large enough relative to the merged in parts) as the same entity.

Now let us cast these ideas into more precise form, and define the following notations:

- A_k k^{th} entity of image I_1;
- B_l l^{th} entity of image I_2;
- S_1 sum of the size of the intersections of A_k with the entities of image I_2, except B_l;
- S_2 sum of the size of the intersections of B_l with the entities of image I_1, except A_k.

If the following inequalities hold at the same time:

$$(S_1 + S_2)/ \mid A_k \cap B_l \mid \; < T_{S1}, \tag{1}$$

$$\mid A_k \cap B_l \mid / \mid A_k \mid \; > T_{S2}, \tag{2}$$

$$\mid A_k \cap B_l \mid / \mid B_k \mid \; > T_{S2}, \tag{3}$$

then entities A_k and B_l are considered as the same entity. Notice that since sameness means a one-to-one relation T_{S2} should be higher than 0.5. The quantities T_{S1} and T_{S2} are setable threshold parameters, their values may depend

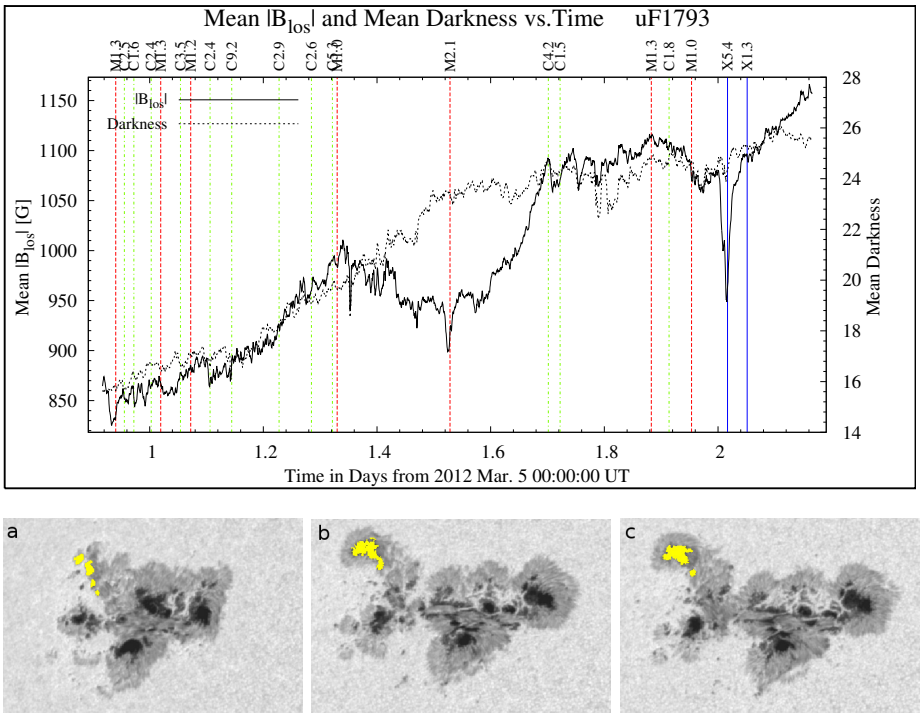

Figure 3. Upper panel, time profile of the absolute value of the LOS mean magnetic induction (solid curve) and the mean darkness (dotted curve) for the umbra family shown on the lower panels at different times (yellow). Note that darkness, by its definition, is a dimensionless quantity, see its definition in Section 4.1.1. The color vertical lines show the times of the flares: dash-dot green, dashed red, and solid blue colors designate C, M, and X classes, respectively. (**a**) 2012 March 5 22:00:29 UT, (**b**) 2012 March 7 00:23:44 UT (X5.4 flare), and (**c**) 2012 March 7 03:58:59 UT.

on the time interval between the two images and the quality of the images. For HMI images with cadence 45 s the value 0.05 was used for T_{S1} and 0.6 for T_{S2}.

2.2. Broad relation

We consider two entities (E_1 and E_2) of the same class in two different images as R_b related if the following inequality holds:

$$\mid E_1 \cap E_2 \mid / \min(\mid E_1 \setminus E_2 \mid, \mid E_2 \setminus E_1 \mid) > T_R. \tag{4}$$

The numerator of Equation (4) requires that some overlap is needed for E_1 and E_2 to be related. The denominator secures that this overlap should be large enough, *i.e.*, the larger part of the smaller entity should be inside the larger entity. The ratio behind this requirement is that during the time elapsed between the exposures of the two images the entities of the second image may move on the solar surface and their sizes may also change causing overlaps that do not mean real merging or splitting (they may be just close neighbors). With the setable threshold parameter T_R, we can say how rigorous we are about false

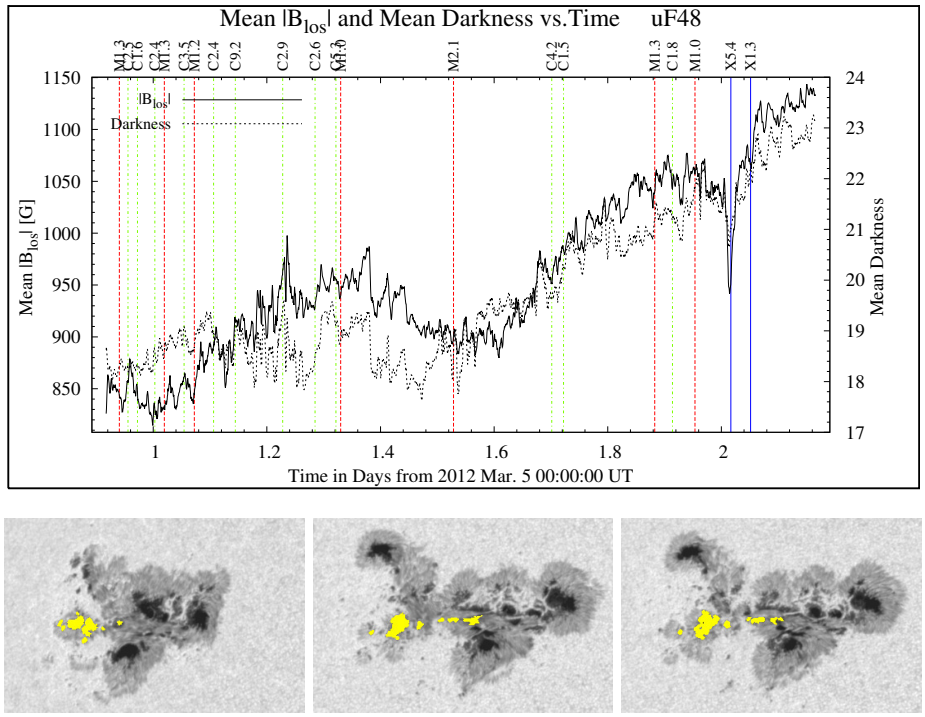

Figure 4. Upper panel, time profile of the absolute value of the LOS mean magnetic induction (solid curve) and the mean darkness (dotted curve) for the umbra family shown on the lower panels at different times (yellow). Note that darkness, by its definition, is a dimensionless quantity, see its definition in Section 4.1.1. The color vertical lines show the times of the flares: dash-dot green, dashed red, and solid blue colors designate C, M, and X classes, respectively. (**a**) 2012 March 5 22:00:29 UT, (**b**) 2012 March 7 00:23:44 UT (X5.4 flare), and (**c**) 2012 March 7 03:58:59 UT.

positives: the higher the value, the more rigorous we are. Its value may depend on the time interval between the two images and the quality of the images. For HMI images with cadence 45 s the value 0.5 is used. Notice that if two entities are related in the R_s sense then they are related in the R_b sense too.

2.3. Broad and sameness relation graphs

After having determined the relations between entities in consecutive images for an image series, a graph can be constructed for each entity-relation pair: the vertexes are the entities in the images and the edges link the entities being related in consecutive images.

The relation graph can be decomposed into connected components. The entities (vertexes) of a connected component comprise an entity family. For any two members of an entity family there exists a path (through the related pairs) connecting the two entities. In this context, families are higher level entities in sunspot groups. Probably a family correspond to a wider branch of the emerging tree of the magnetic flux strands (Piddington, 1979).

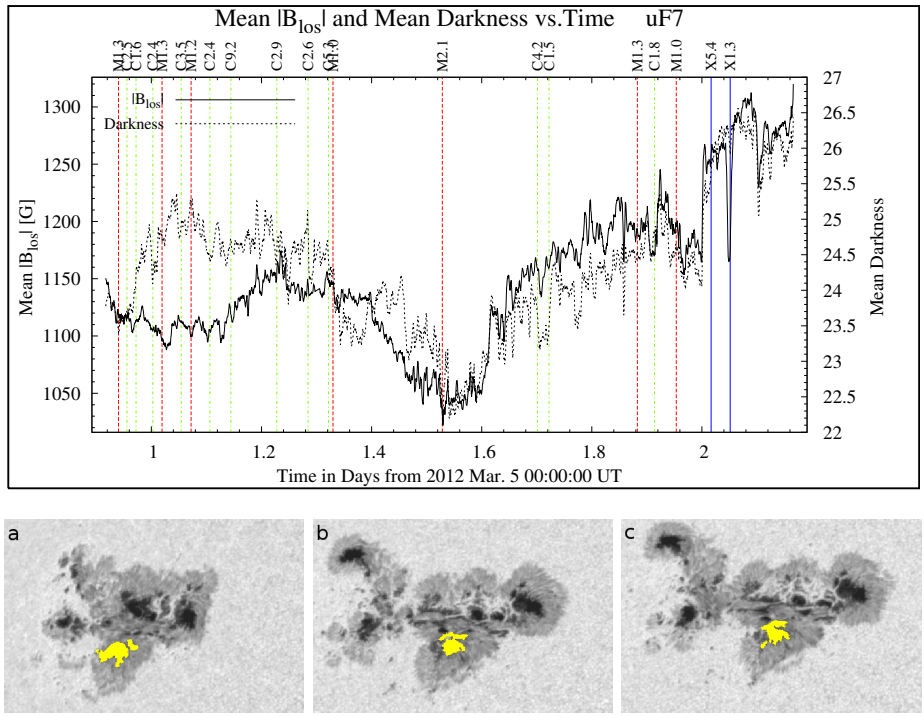

Figure 5. Upper panel, time profile of the absolute value of the LOS mean magnetic induction (solid curve) and the mean darkness (dotted curve) for the umbra family shown on the lower panels at different times (yellow). Note that darkness, by its definition, is a dimensionless quantity, see its definition in Section 4.1.1. The color vertical lines show the times of the flares: dash-dot green, dashed red, and solid blue colors designate C, M, and X classes, respectively. (**a**) 2012 March 5 22:00:29 UT, (**b**) 2012 March 7 00:23:44 UT (X5.4 flare), and (**c**) 2012 March 7 03:58:59 UT.

Those members of a family that are in the same image of an image series comprise a generation of the family, *i.e.*, we have as many generation as the number of those images that have at least one member of the family. As we partitioned sunspot group entities into families for a solar image series, now we partition a family into generations. For example, the three white-light solar images in Figure 6 show three generations of an umbra family (R_b relation), the umbrae of the family are shown in yellow color.

The notation of the generation is especially useful when the families are based on the broad relation. In this case, not the property (*e.g.*, position, area, magnetic field, and intensity) of an individual entity (pore, spot, umbra, and penumbra) is used (followed) but the property is averaged over the members of the generation, *i.e.*, if we want to follow how a property evolves with time for a family, we partition the family into generations and for each generation determine the average of the property and follow this average for the image series.

Iterating through the members of a family the mergings, fragmentations, and splittings of the entities can be studied.

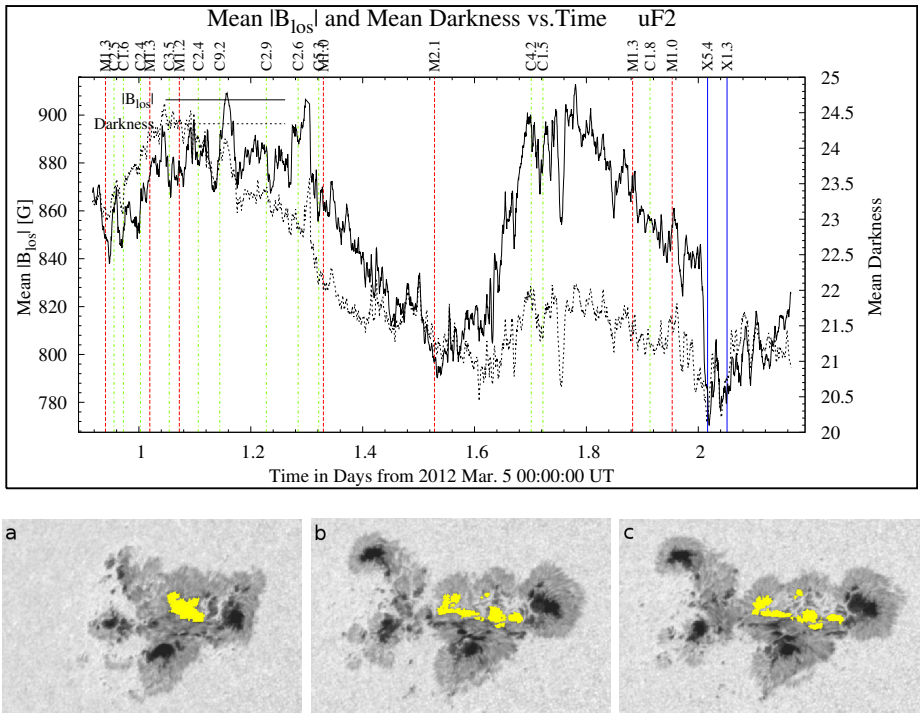

Figure 6. Upper panel, time profile of the absolute value of the LOS mean magnetic induction (solid curve) and the mean darkness (dotted curve) for the umbra family shown on the lower panels at different times (yellow). Note that darkness, by its definition, is a dimensionless quantity, see its definition in Section 4.1.1. The color vertical lines show the times of the flares: dash-dot green, dashed red, and solid blue colors designate C, M, and X classes, respectively. (**a**) 2012 March 5 22:00:29 UT, (**b**) 2012 March 7 00:23:44 UT (X5.4 flare), and (**c**) 2012 March 7 03:58:59 UT.

3. Observation and data processing

3.1. Observation

To demonstrate the usage of the proposed method we applied it for tracking the magnetic and intensity properties of the umbra families in a $\beta\gamma\delta$ sunspot group, NOAA 11429. The intensity images and magnetograms were taken by the *Helioseismic and Magnetic Imager* (HMI; Schou *et al.*, 2012) with 45s cadence on board *Solar Dynamics Observatory* (SDO; Pesnell, Thompson, and Chamberlin, 2012). The GOES flare times and positions were downloaded from the website http://www.solarmomitor.org. All the images between 2012 March 4 00:00:00 and 8 00:00:00 UT were processed but, in order to see enough details in the figures, only parts of this time interval are plotted in several figures. There is a gap in the SDO/HMI images between 2012 March 7 06:56:44 and 07:29:15 UT, therefore family data are plotted mostly up to the start of this gap.

3.2. Data processing

A project was undertaken in order to create automatically such a sunspot database that can be used to automatically study the time development of various properties of different entities of sunspot groups. The entities included are: sunspot group (as whole), spot (as a whole: penumbra + umbrae), penumbra (as whole), umbra (as whole), and families (umbra family, same umbra family, spot family, and same spot family). The properties included are: area, position, intensity, and magnetic field (mean, flux). This aim is achieved by a pipeline of programs: *SAM*, *RELATE*, *TRACK*, *PLOT*, and *ANALYZE*.

SAM (Sunspot Automatic Measurement, Győri (1998)) finds sunspots in solar images and creates the base part of a database containing the following data:

- The pixel domain of each umbra and of each spot (as a whole: penumbra + umbrae). Penumbral domain can be deduced from the spot domain and the domains of the umbrae it contains.
- The containment relations: which spot contains which umbrae.
- The area for each umbra and for each spot. Penumbral area can be deduced from the spot area and the area of the umbrae it contains.
- The position (in pixel and in heliographic coordinates) of the center-of-mass for each umbra and for each spot.
- The intensity measured from the quiet Sun intensity in the standard deviation of the quiet Sun intensity.
- The magnetic field (if available) for each umbra and for each spot. Two types of the magnetic field are provided: the mean field and the flux.

An example of the sunspot (umbra and penumbra) boundaries determined by *SAM* can be seen in Figure 1.

RELATE expands the spot database with data that relate entities of the first image to the entities of the second image for a consecutive image pair. Since we have two entities (umbrae and spots) and two relations (R_b and R_s) this means four data fields.

TRACK expands the spot database with data that classify the same type of entities of an image series into families, *i.e.*, determines which entity for a given relation belongs to which family of the image series. Since we have two entities (umbrae and spots) and two relations (R_b and R_s) this means four data fields.

PLOT creates the time evolution data for different properties of various families and plots them.

ANALYZE analyzes the time evolution data created by *PLOT*, *i.e.*, determines trends and their properties, and finds regional extrema and establishes their properties.

4. Results

4.1. Flare related-changes in magnetic field and intensity

Figures 3 - 6 show the time evolution of the line-of-sight (LOS) mean magnetic field (mean magnetic flux density) for the four largest umbra families of sunspot group 11429. These families are based on relation R_b.

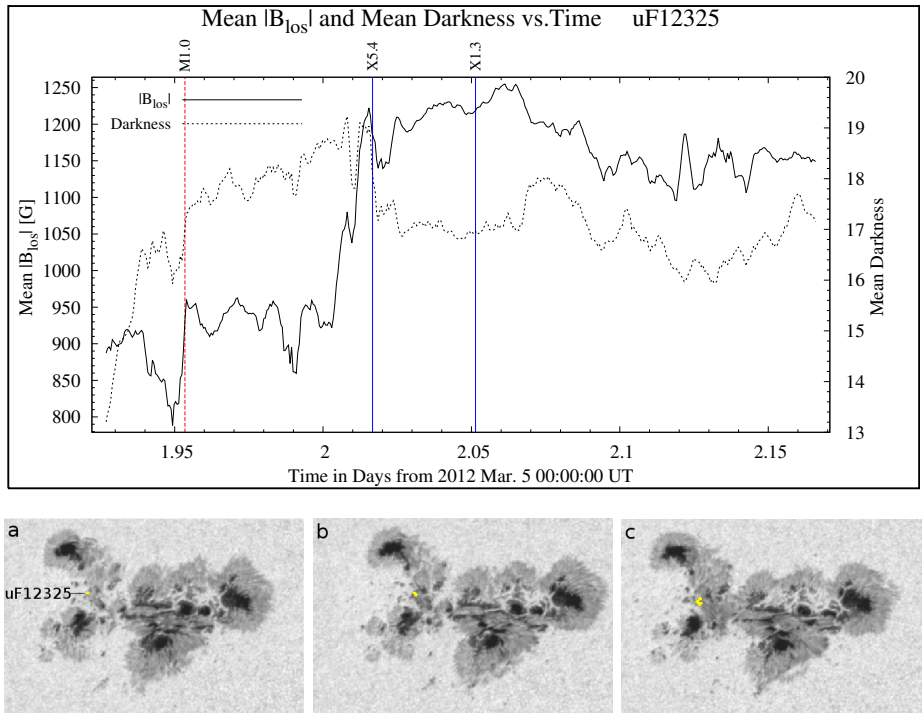

Figure 7. Upper panel, time profile of the absolute value of the LOS mean magnetic induction (solid curve) and the mean darkness (dotted curve) for the umbra family shown on the lower panels at different times (yellow). Note that darkness, by its definition, is a dimensionless quantity, see its definition in Section 4.1.1. The color vertical lines show the times of the flares: dash-dot green, dashed red, and solid blue colors designate C, M, and X classes, respectively. (**a**) 2012 March 6 22:13:59 UT, (**b**) 2012 March 7 00:23:44 UT (X5.4 flare), and (**c**) 2012 March 7 03:58:59 UT.

The upper panels of Figure 3 and Figure 4 show sharp regional minima with high depth at the X5.4 flare peak time (2012 March 7 00:24 UT) for the umbra families shown on the lower panels of the figures. Similarly, the upper panel of Figure 5 shows a sharp regional minimum with high depth at the X1.3 flare peak time (2012 March 7 01:14 UT) for the umbra family shown on the lower panel of the figure. Notice that this is the umbra family being nearest to the X1.3 class flare (see Figure 2).

The depth of this minimum is large relative to the depth of other regional minima. It can also be seen that, after the flare, the magnetic field is rapidly restored to the value before the flare and the trend of the magnetic field evolution generally continues as before. The value of this transient decrease of the absolute magnetic field amounts to about 100 Gauss. These families are of negative polarity.

For the umbra family shown in Figure 6 the sudden decrease in the absolute magnetic field (also about 100 Gauss) is also present. However the recovery is much slower.

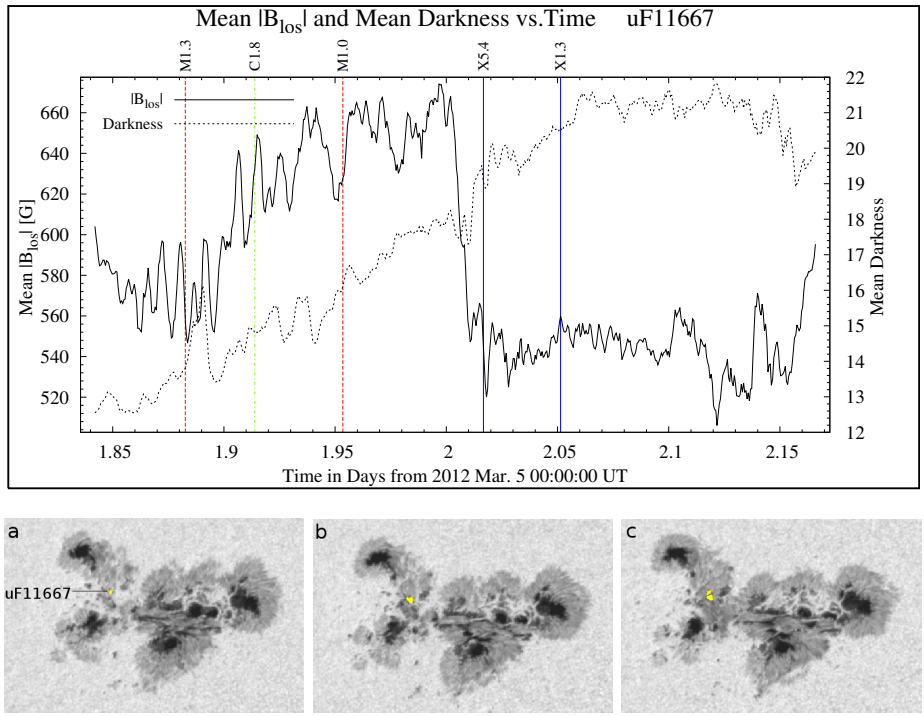

Figure 8. Upper panel, time profile of the absolute value of the LOS mean magnetic induction (solid curve) and the mean darkness (dotted curve) for the umbra family shown on the lower panels at different times (yellow). Note that darkness, by its definition, is a dimensionless quantity, see its definition in Section 4.1.1. The color vertical lines show the times of the flares: dash-dot green, dashed red, and solid blue colors designate C, M, and X classes, respectively. (**a**) 2012 March 6 20:11:44 UT, (**b**) 2012 March 7 00:23:44 UT (X5.4 flare), and (**c**) 2012 March 7 03:58:59 UT.

Thoroughly examining the magnetic field curves in the figures it is also found that several regional extrema also coincide with flares or are near them (see for example the M2.1 flare, 2012 March 6 12:41 UT), but not all of them, and *vice versa*. Probably, the smaller the flare, the more the distance between the family and the flaring position matters. This needs further investigations.

A definition is in order: the darkness (D) of a pixel of a solar image is measured from the mean intensity of the quite Sun (I_{qs}) using as unit the standard deviation (σ) of the mean intensity of the quite Sun ((*i.e.*, $D = (I_{qs} - I)/\sigma$, where I is the intensity). Quiet Sun is defined as the part of the solar image that contains no solar features except solar granulation. The advantage of this definition is that it is invariant against the intensity transformation $I_t = aI + b$, where I is the intensity, I_t the transformed intensity, and a and b are constants. This type of transformation may occur during image acquisition and preprocessing.

In the case of the two most complex umbra families (Figure 4 and Figure 6), the trend of the darkness curves follows the trend of the absolute magnetic field curves. However, for the other umbra families (Figure 3, Figure 5, the trend of the darkness and magnetic field curves differs in certain time intervals significantly.

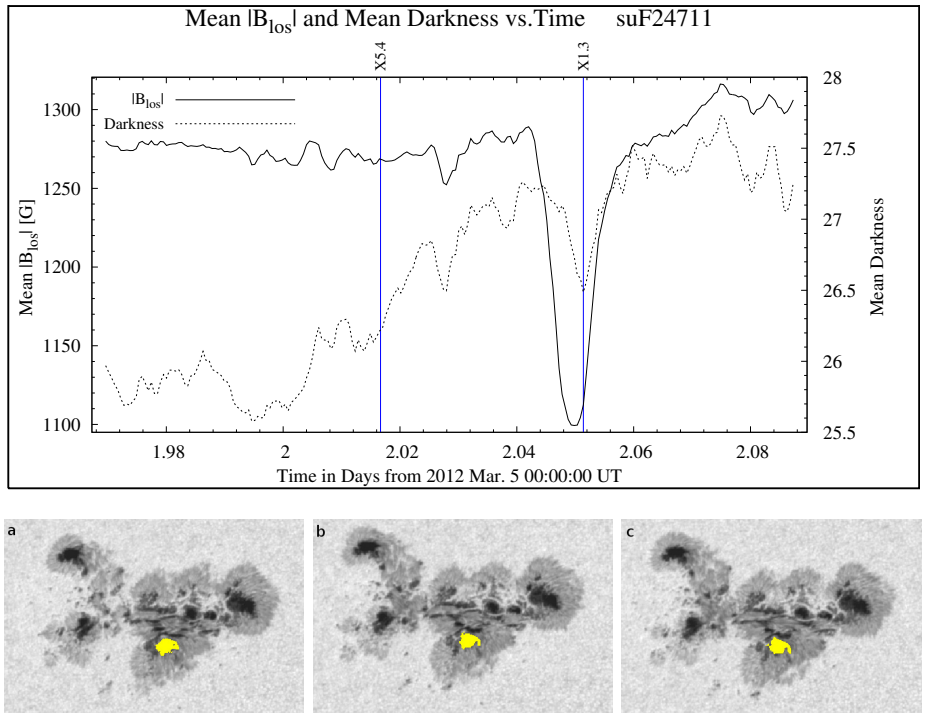

Figure 9. Upper panel, time profile of the absolute value of the LOS mean magnetic induction (solid curve) and the mean darkness (dotted curve) for the same umbra shown on the lower panels at different times (yellow). Note that darkness, by its definition, is a dimensionless quantity, see its definition in Section 4.1.1. The blue vertical lines show the times of the X-class flares. (**a**) 2012 March 6 23:15:29 UT, (**b**) 2012 March 7 01:13:59 UT (X1.3 flare), and (**c**) 2012 March 7 02:05:44 UT.

Now, after the largest umbra families, let us choose two newly emerging small ones (area < 3.5 mh). They begin to emerge about 2 hours before the X5.4 flare and are shown in Figure 7 and Figure 8. They are located on the opposite sides of the polarity inversion line very near to each other (see left panel of Figure 2). The absolute magnetic field of the negative polarity umbra in Figure 7 increased by 260 Gauss in 21 minutes. This change was not transient-like as it was for the large negative-polarity umbra families discussed above: the magnetic field roughly kept its new value after the flare. The absolute magnetic field change of the positive polarity umbra in Figure 8 behaved the other way: the magnetic field decreased by 120 Gauss in 21 minutes. However, the new magnetic field value is also roughly kept after the flare.

As for the darkness curves in Figure 7 and Figure 8, they also behave differently. The darkness of the the umbra family shown in Figure 7 increased rapidly with more or less fluctuations until the onset of the flare X5.4, during the flare its value rapidly decreased by 7 percents, and after the flare, a slow decrease commenced with more or less fluctuations. The darkness of the umbra family shown in Figure 8 increased, with some fluctuations, before the flare X1.3. However, after the flare, its value remained more or less constant. A small (in

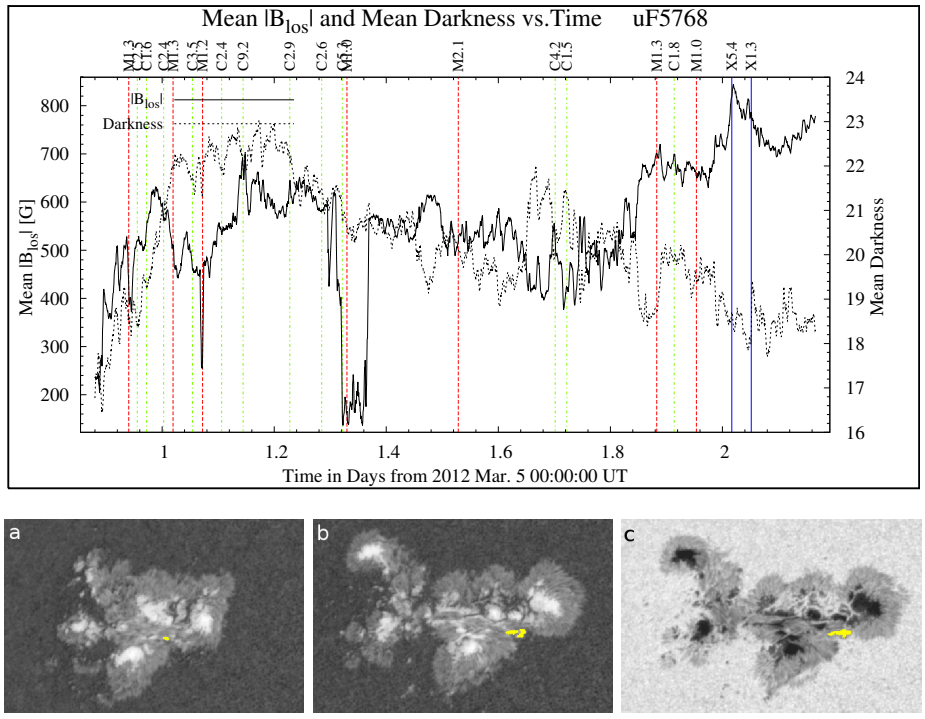

Figure 10. Upper panel, time profile of the absolute value of the LOS mean magnetic induction (solid curve) and the mean darkness (dotted curve) for the same umbra shown on the lower panels at different times (yellow). Note that darkness, by its definition, is a dimensionless quantity, see its definition in Section 4.1.1. The color vertical lines show the times of the flares: dash-dot green, dashed red, and solid blue colors designate C, M, and X classes, respectively. (**a**) 2012 March 5 22:00:29 UT, (**b**) 2012 March 7 00:23:44 UT (X5.4 flare), and (**c**) 2012 March 7 03:59:44 UT.

the order of other fluctuations along the curve) transient decrease can be seen at the time of the X5.4 flare.

Figure 9 depicts temporal variation in the absolute value of the LOS mean magnetic field and in the darkness of the same umbra (R_s relation). During the X1.3 flare a deep (175 G), well-like minimum developed in the absolute magnetic field. After the flare, the magnetic field has restored the value it had before the flare. The darkness of the umbra also exhibited transient variations during the X1.3 flare. It is noteworthy that there is no sign of the effect of the larger X5.4 flare on this umbra.

Figure 10 depicts an umbra family that shows flare-related abrupt magnetic field changes with several different classes of flares. The ones with the most significant changes are: M1.3 on 2012 March 5 at 22:34, M1.2 on 2012 March 6 at 01:44, C5.3 on 2012 March 6 at 07:43, M1.0 on 2012 March 6 at 07:55, X5.4 on 2012 March 7 at 00:24, X1.3 on 2012 March 7 at 01:14. This umbra family was a part of a positive polarity, long, narrow wedge (see the bottom row of Figure 1) intruding (emerging) into a negative polarity penumbral domain.

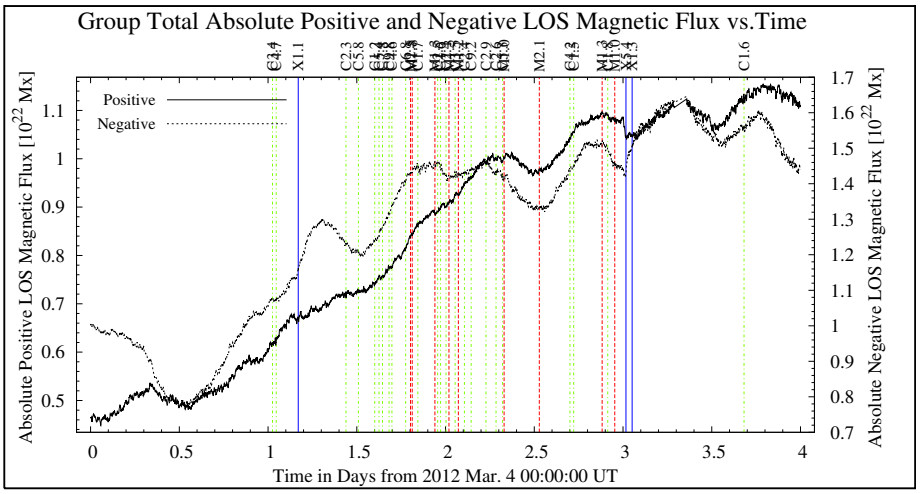

Figure 11. The group's total positive (solid curve) and negative (dotted curve) LOS magnetic fluxes as function of time. The color vertical lines show the times of the flares: dash-dot green, dashed red, and solid blue colors designate C, M, and X classes, respectively.

We conjecture that this umbra family was not only the enduring location of the flares associated with it but, at least partly, the triggering cause of these flares.

Hitherto we have studied the magnetic field at medium (large umbra families) and at small (small umbra families and same umbra) spatial scales. Let us see now how the magnetic flux evolves at larger scale, that is, at the scale of the sunspot group itself. Figure 11 shows the time profiles of the group's total absolute positive and negative magnetic fluxes separately. There is a trend of increasing fluxes with time for both of the curves. However, especially after March 6, a quasi-periodic change is superimposed on this trend. It is at the sharpest local minimum of this quasi-periodic change where the X5.4 flare occurred. It is also interesting to observe that the negative absolute flux is on average larger by 45 percent than the positive one.

4.2. Flare-related changes in motion

Now let us see the motions of the umbra families, since these can deform the magnetic field of a sunspot group the way that magnetic energy accumulates in it, and this energy is converted into other forms by a flare.

Figure 12 shows how the distance between the opposite polarity umbra families uF2 (see Figure 6) and uF7 (see Figure 5) changes with time. We can observe a nearly uniform, three days long convergence of the two families, at least until the two X class flares (X5.4 and X1.3) happen. These flares are produced at the turning point for the motion. The decrease in the distance in three days was quite large (1.5^o, about 50 percent). After the flares, the two families begin to diverge. This divergence has been sustaine for 5 hours when, unfortunately, there was a gap in the observation. A square pulse decrease in the distance of the two

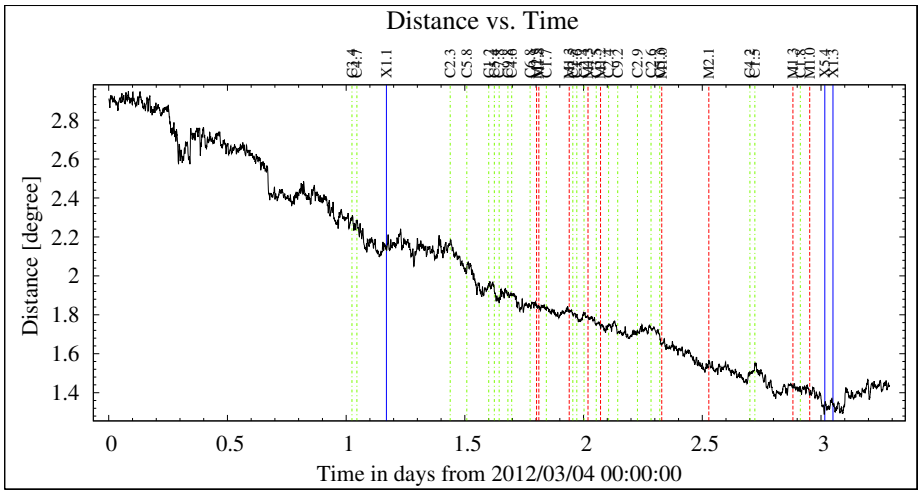

Figure 12. Distance between uF2 and uF7 umbra families as function of time. The color vertical lines show the times of the flares: dash-dot green, dashed red, and solid blue colors designate C, M, and X classes, respectively.

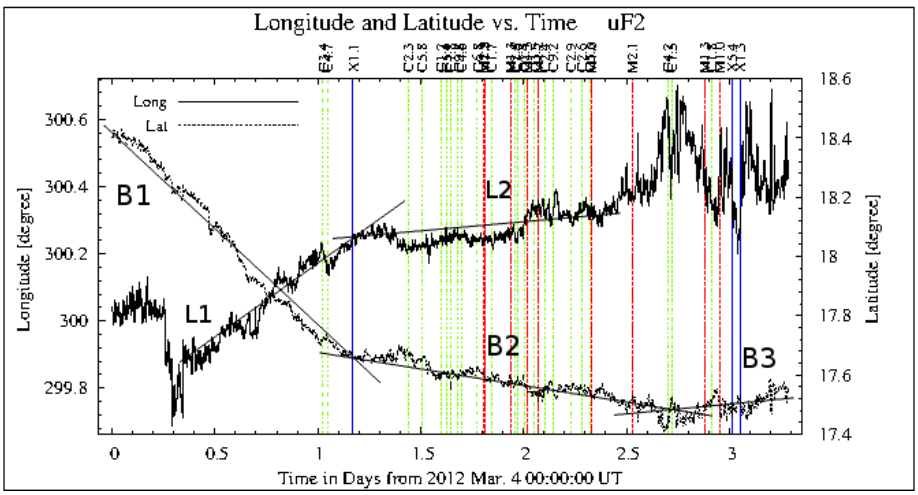

Figure 13. Heliographic longitude (solid curve) and latitude (dotted curve) of the uF2 umbra family as function of time. The color vertical lines show the times of the flares: dash-dot green, dashed red, and solid blue colors designate C, M, and X classes, respectively.

umbra familes, located around the times of the two flares (X5.4 and X1.3) can also be observed.

Figure 13 depicts the heliographic longitude (L) and latitude (B) as function of time for the uF2 umbra family. During three days, uF2 moved westwards in L with the average speed of $0.15^o/d$. This movement is not uniform: it has intervals of larger fluctuations and intervals of linear trends (L1 and L2, shown by solid straight lines in Figure 13) with different slopes. A look at Figure 13

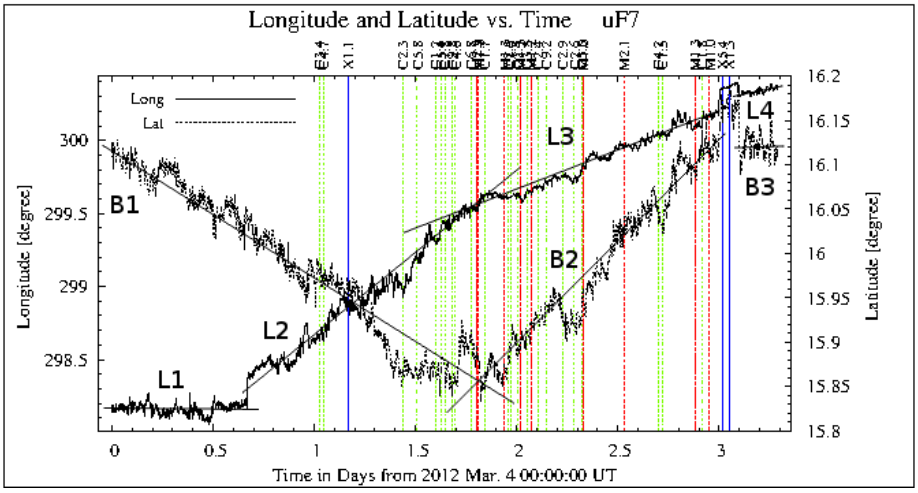

Figure 14. Heliographic longitude (solid curve) and latitude (dotted curve) of the uF7 umbra family as function of time. The color vertical lines show the times of the flares: dash-dot green, dashed red, and solid blue colors designate C, M, and X classes, respectively.

reveals that the X1.1 (2012 March 5 04:05 UT) flare can be associated with a change in linear trends L1 and L2, *i.e.*, with a break point in the L motion curve. Moreover, abrupt transient decreases in L happen at the times of the following flares: C1.5, 2012 March 6 17:20 UT; C1.8, 2012 March 6 21:56 UT; X5.4, 2012 March 7 00:24 UT; X1.3, 2012 March 7 01:14 UT.

Now turning to the movement in B we can observe three linear trends (B1, B2, and B3, solid straight lines in Figure 13). The B1 and the B2 trends represent southward movement: the B1 has high slope ($0.76^o/d$) and the B2 has low one ($0.16^o/d$). The X1.1 flare can be associated with a break point in the (B) motion curve, *i.e.*, with a change in linear trends B1 and B2. The B3 linear trend begins at the turning point of the motion, *i.e.*, where it turns to northwards. Two C class flares (C1.5, 2012 March 6 17:20 UT and C4.2, 2012 March 6 16:50 UT) coincide with this turning point.

Figure 14 depicts the temporal evolution of the heliographic longitude and latitude for the uF7 umbra family. uF7 moved westwards in L with an average speed of $0.64^o/d$. The L motion curve can be broken down into five intervals: four of them have linear trends (L1, L2, L3, and L4 shown by solid straight lines in Figure 14), and the fifth one shows a square pulse increase in L around the times of the X5.4 and the X1.3 flares. One of the break points of the L motion curve (the one where L2 and L3 linear trends meet) coincides and is co-spatialwith two close M class flares (M2.5, 2012 March 5 19:16 UT and (M1.8, 2012March 5 19:30 UT).

The B motion curve can be separated into four parts: three of them (B1, B3, and B3) exhibit linear trends (fitted by solid straight lines in Figure 14) and the fourth one shows transient increase in B for both of the flares X5.4 and X1.3. At first uF7 moves southwards (away from uF2) in B with an average speed of

$0.15^o/d$ then it takes a turn and move northwards (towards uF2) with an average speed of $0.22^o/d$. The turning point can be associated with the same two M class flares (M2.5 and M1.8) as was the case for the L motion curve. Shortly after the X1.3 flare the motion in B has stopped for 5 hours when, unfortunately, there was a gap in the observation (see B3).

It is worth mentioning that, although both families move westwards, their speeds are very different, uF7 move about four times faster than uF2. This means that they result in increasing magnetic shear, which is a favorable situation for flares, especially when there is a converging motion too, as the case is here.

5. Discussion and Conclusion

A method was developed to relate sunspot group entities in consecutive solar images. This relation serves two purposes simultaneously, namely to group the sunspot group entities into families and to track these families. The method was applied to track the evolution of the LOS magnetic field and the intensity (darkness) of the umbra families of NOAA AR 11429 with special attention to the X5.4 flare released in this sunspot group.

The LOS magnetic field changes for umbra families shown in Figures 3-5 are transient-like: they begin to rapidly decrease at the onset of the flare, reach their minima at the flare peak time and then begin rapidly increasing and, for the end of the flare, recover the value before the flare.

Similar behavior was reported by Kosovichev and Zharkova (2001). They studied the X5.7 flare of 2000 July 4 in AR NOAA 9077 ("Bastille Day Flare") and found abrupt variations of the LOS magnetic field and the intensity in seven rectangular regions. This behavior was classified by them as transient change and is quite similar to those found by us for the umbra families. They explained this transient change by high-energy electrons bombarding the solar surface.

If we have a thorough look at the magnetograms in the bottom row of Figure 1 we will discern an interesting situation: the large umbrae of umbra family uF1793 (Figure 3) and uF48 (Figure 4) exhibit patches of weak longitudinal magnetic field and a few pixels of these patches have opposite polarity with respect to the umbral magnetic field. We have also seen before that these families show magnetic transients. Transient sign reversal of the magnetic polarities was also reported by Patterson and Zirin (1981) during the two large flares on 1979 November 5 and by Qiu and Gary (2003) during the impulsive phase of an X5.6 flare on 2001 April 6. Qiu and Gary (2003) observed that the transient sign reversal was co-spatial with the strong hard X-ray emission and that the time development of reversed magnetic flux coincided with the hard X-ray emission peak and showed a similar temporal evolution.

Probably these transients could be attributed to the highly energetic electron beam accelerated in the flare and precipitated in the chromosphere and also to changes in the line profile used to determine the magnetic field, in some cases so drastic that the line turns into emission. This effect is especially significant in the case of a dark umbra. This situation adversely influences the accuracy of the method used for determining the magnetic field during the flare. For detailed

description of this mechanism see Ding, Qui, and Wang (2002) and Qiu and Gary (2003). The transients related to the X1.3 flare and shown by the umbra family uF7 (Figure 5) and by its main umbra (suF24711, Figure 9), also fall in this category. It is noteworthy that Ding, Qui, and Wang (2002) and Qiu and Gary (2003) used, in their studies, the Ni I 676.8 nm line, which was used to create SOHO/MDI (*Solar and Heliospheric Observatory's Michelson Doppler Imager*) magnetograms, while SDO/HMI observes in the Fe I 617.3 nm line.

Figure 6, Figure 7, and Figure 8 show rapid magnetic field changes related to the X5.4 flare. These are not transient but step-wise (irreversible). They can be explained by the back-reaction on the photospheric magnetic field. Estimating the work done by the Lorentz forces, arising from the flare, on the photosphere, Hudson, Fisher, and Welsh (2008) and Fisher *et al.* (2012) have predicted that after the flare the photospheric magnetic fields become more horizontal as back-reaction for the flare. There are flare models (*e.g.*, Melrose (1997) and Moore *et al.* (2001)) that predict the appearance of low-lying field lines after the flare, which also means that the photospheric magnetic fields become more horizontal after the flare. Several authors (see the Introduction) have reported flare-associated, irreversible changes in the magnetic fields of various active regions.

Several favorable factors for flares met in AR 11429: converging same- and opposite-polarity umbrae, shearing motions of opposite-polarity umbrae, emerging umbrae in the vicinity of the PIL, high magnetic gradients along the PIL, and the fragmentation of the umbrae that take part in the converging motion. The converging and shearing motion of umbra families uF2 and uF7 towards the PIL and towards each other (Figure 12, Figure 13, and Figure 14) may provide the driving for the flares that occurred along the PIL as it was shown by Amari *et al.* (2003) in MHD simulation. New flux emergence (*e.g.*, Figure 7, Figure 8 and Figure 10) and flux (umbra) fragmentation (Figure 6) increase the topological complexity of the AR. It was shown in several papers that the topological complexity is a determining parameter in flare productivity (Mandrini *et al.* (1991); Démoulin, Hénoux, and Mandrini (1992) Mandrini *et al.* (1993);). By increasing the topological complexity, the newly emerging (next to the opposite polarity uF2) and rapidly developing umbra family uF1763 might also contribute the energy build up for the X5.4 flare that happened at a sharp corner of the PIL.

Several authors observed flare-related changes in sunspot motions and in photospheric flows (for references see the Introduction). For example, Anwar *et al.* (1993) pointed out rapid motion of a sunspot during the X1.1 flare on November 15 1991 and interpreted it as driven by the Lorentz force created by the flare. In this paper we found that the break and turning points in the motions of certain umbra families are associated with flares.

Umbra family uF5768 (Figure 10) and a prolongation of umbra family uF48 (Figure 4) emerged between umbra families uF2 (Figure 6) and uF7 (Figure 5). These emergence episodes might be the cause of the break and the turning points in the motion curves of the umbra families uF2 (Figure 13) and uF7 (Figure 14) and also might provide the trigger for several flares.

An additional possible explanation for the break and the turning points in the motion of the umbra families might be the Lorentz force created as a back reaction to the flare and acting on the photosphere (Fisher *et al.* (2012)). Studying the X2.2 flare on 2011 February 15, Petrie (2013) finds significant torsional Lorentz force changes during the flare and Lorenz force shear along the PIL. Wang *et al.* (2014), also studying the X2.2 flare on 2011 February 15, found that two sunspots showed sudden acceleration of rotational motion during the flare. They concluded that it was the change of the Lorentz force that drove this sudden motion.

Flare-related changes were found at every spatial scale (small umbra families, same umbra, large umbra families, and entire group) of the sunspot group studied in this paper. However this does not mean that every entity of the sunspot group manifested changes associated with a given flare, *e.g.*, the umbra depicted in Figure 9 showed large variations during the X1.3 flare but nothing during the larger X5.4 flare.

It is worth mentioning that many more umbra families and same umbra families exhibited some kind of the abrupt magnetic field changes, mainly the ones located close to the PIL, than it was possible to include in this paper.

Acknowledgments The author would like to thank the referee and the editor for comments that helped improve this manuscript. SDO images are courtesy of *Solar Dynamic Observatory* (NASA). The GOES "X-ray Flare" dataset was prepared by and made available through the NOAA National Geophysical Data Center (NGDC). The GOES X-ray flare times and positions data are supplied courtesy of SolarMonitor.org. The research leading to these results has received funding from the European Commissions Seventh Framework Programme (FP7/2007-2013) under the grant agreement eHEROES (project number 284461).

References

Amari, T., Luciani, J.F., Aly, J.J., Mikic, Z., Linker, J.: 2003, Coronal mass ejection: Initiation, magnetic helicity, and flux ropes. I. Boundary motiondriven evolution. *Astrophys. J.* **585**, 1073. DOI. [Amari_ApJ_2003_585]

Anwar, B., Acton, L.W., Hudson, H.S., Makita, M., McClymont, A.N., Tsuneta, S.: 1993, Rapid sunspot motion during a major solar flare. *Solar Phys.* **147**, 287. DOI. [Anwar_1993_SoPh_147_287-303]

Brown, D.S., Nightingale, R.W., Alexander, D., Schrijver, C.J., Metcalf, T.R., Shine, R.A., Title, A.M., Wolfson, C.J.: 2003, Observations of rotating sunspots from TRACE. *Solar Phys.* **216**, 79. DOI. [Brown_2003_SoPh_216]

Démoulin, P., Hénoux, J.C., Mandrini, C.H.: 1992, Development of a topological model for solar flares. *Solar Phys.* **139**, 105. DOI. [Demoulin_1992_SoPh_139]

Deng, N., Liu, C., Yang, G., Wang, H., Denker, C.: 2005, Rapid penumbral decay associated with an X2.3 flare in NOAA Active Region 9026. *Astrophys. J.* **623**, 1195. DOI. [Deng_2005_ApJ_623]

Dezső, L., Gesztelyi, L., Kondás, L., Kovács, A., Rostás, S.: 1980, Motions in the solar atmosphere associated with the white light flare of 11 July 1978. *Solar Phys.* **67**, 317. DOI. [Dezso80]

Ding, M.D., Qui, J., Wang, H.: 2002, Non-LTE calculation of the Ni I 676.8 nanometer line in a flaring atmosphere. *Astrophys. J. Lett.* **576**, L83. DOI. [Ding_2002_ApJL_576]

Fisher, G.H., Bercik, D.J., Welsch, B.T., Hudson, H.S.: 2012, Global forces in eruptive solar flares: The Lorentz force acting on solar atmosphere and solar interior. *Solar Phys.* **277**, 59. DOI. [Fisher_SoPh_2012_277]

Gosain, S.: 2012, Evidence for collapsing fields in the corona and photosphere during the 2011 February 15 X2.2 flare: SDO/AIA and HMI observations. *Astrophys. J.* **749**, 85. DOI. [Gosain_ApJ_2012_749]

Gosain, S., Venkatakrishnan, P., Tiwari, S.K.: 2009, Hinode observations of coherent lateral motion of penumbral filaments during an X-class flare. *Astrophys. J. Lett.* **706**, L240. DOI. [Gosain_2009_ApjL_706]

Győri, L.: 1998, Automation of area measurement of sunspots. *Solar Phys.* **180**, 109. DOI. [Gyori88]

Hagenaar, H.J., Schrijver, C.J., Title, A.M., Shine, R.A.: 1999, Dispersal of magnetic flux in the quiet solar photosphere. *Astrophys. J.* **511**, 932. DOI. [Hagenaar_ApJ_1999_511]

Hudson, H.S., Fisher, G.H., Welsh, B.T.: 2008, In: Howe, R., Komm, R.W., Balasubramaniam, K.S., Petrie, G.J.D. (eds.) *Subsurface and Atmospheric Influences on Solar Activity*, ASP. Conf. Ser. 383, 221. [Hudson2008]

Kosovichev, A.G., Zharkova, V.V.: 2001, Magnetic energy release and transients in the solar flare of 2000 July 14. *Astrophys. J. Lett.* **550**, L105. DOI. [Kosovichev_ApJL_2001_550]

Liu, C., Deng, N., Liu, Y., Flconer, D., Goode, P.R., Denker, C., Wang, H.: 2005, Rapid change of spot structure associated with seven major flares. *Astrophys. J.* **622**, 722. DOI. [Liu_2005_ApJ_622]

Liu, C., Deng, N., Liu, R., Lee, J., Wiegelmann, T., Wang, H.: 2012, Repid changes of photospheric magnetic field after tether-cutting reconnection and magnetic implosion. *Astrophys. J. Lett.* **745**, L4. DOI. [Liu_ApJL_2012_745]

Mandrini, C.H., Démoulin, P., Hénoux, J.C., Machado, M.E.: 1991, Evidence for the interaction of large scale magnetic structures in solar flares. *Astron. Astrophys.* **250**, 541. [Mandrini_1991_AA_250]

Mandrini, C.H., Rovira, M.G., Démoulin, P., Hénoux, J.C., Machado, M.E., Wilkinson, L.K.: 1993, Evidence for magnetic reconnection in large-scale magnetic structures in solar flares. *Astron. Astrophys.* **272**, 609. [Mandrini_1993_AA_272]

Melrose, D.B.: 1997, A solar flare model based on magnetic reconnection between current-carrying loops. *Astrophys. J.* **486**, 521. [Melrose_ApJ_1997_486]

Moore, R.L., Sterling, A.C., Hudson, H.S., Lemen, J.R.: 2001, Onset of the magnetic explosion in solar flares and coronal mass ejections. *Astrophys. J.* **552**, 833. [Moore_ApJ_2001_552]

Murray, S.A., Bloomfield, D.S., Gallagher, P.T.: 2012, The evolution of sunspot magnetic fields associated with a solar flare. *Solar Phys.* **277**, 45. DOI. [Murray_SoPh_2012_277]

Patterson, A., Zirin, H.: 1981, Transient magnetic field changes in flares. *Astrophys. J. Lett.* **243**, L99. DOI. [Patterson_ApJL_1981_243]

Pesnell, W.D., Thompson, B.J., Chamberlin, P.C.: 2012, The Solar Dynamics Observatory (SDO). *Solar Phys.* **275**, 3. DOI. [Pesnell_2012_SoPh_275]

Petrie, G.J.D.: 2013, A spatio-temporal description of the abrupt changes in the photospheric magnetic and Lorentz-force vectors during the 15 February 2011 X2.2 flare. *Solar Phys.* **287**, 415. DOI. [Petrie_2013_SoPh_287_415-440]

Petrie, G.J.D., Sudol, J.J.: 2010, Abrupt longitudinal magnetic field changes in flaring active regions. *Astrophys. J.* **724**, 1218. DOI. [Petrie_ApJ_2010_724]

Piddington, J.H.: 1979, Solar flares - models and predictions of the flux-rope theory. *Astrophys. J.* **233**, 727. DOI. [Piddington_1979_ApJ_233]

Qiu, J., Gary, D.E.: 2003, Flare-related magnetic anomaly with a sign reversal. *Astrophys. J.* **599**, 615. DOI. [Qiu_ApJ_2003_599]

Raman, K.S., Ramesh, K.B., Selvendran, R.: 2003, The role of sunspot unbral rotation in triggerig solar flares. *Bull. Astr. Soc. India* **31**, 101. [Raman_2003_BASI_31]

Schmieder, B., Hagyard, M.J., Guoxiang Ai, Zhang, H., Kálman, B., Győri, L., Rompolt, B., Demoulin, P., Machado, M.E.: 1994, Relationship between magnetic field evolution and flaring site in AR 6659 in June 1991. *Solar Phys.* **150**, 199. DOI. [Schmieder_1994_SoPh_150]

Schou, J., Scherrer, P.H., Bush, R.I., Wachter, R., Couvidat, S., Rabello-Soares, M.C., et al.: 2012, Design and ground calibration of the Helioseismic and Magnetic Imager (HMI) instrument on the Solar Dynamic Observatory (SDO). *Solar Phys.* **275**, 229. DOI. [Schou_2012_SoPh_275]

Strous, L.H., Scharmer, G., Tarbell, T.D., Title, A.M., Zwaan, C.: 1996, Phenomena in an emerging active region. I. Horizontal dynamics. *Astron. Astrophys.* **306**, 947. [Strous_AA_1996_306]

Tan, C., Chen, P.F., Abramenko, V., Wang, H.: 2009, Evolution of optical penumbral and shear flows associated with the X3.4 flare of 2006 December 13. *Astrophys. J.* **690**, 1820. DOI. [Tan_2009_ApJ_690]

Vemareddy, P., Ambastha, A., Maurya, R.A.: 2012, On the role of rotating sunspots in the activity of solar active region NOAA 11158. *Astrophys. J.* **761**, 60. DOI. [Vemareddy_2012_ApJ_761]

Wang, H., Liu, C.: 2011, In: Choudhary, D.P., Strassmeier, K.G. (eds.) *The Physics of Sun and Star Spots*, Proceedings IAU Symposium No. 273, 15. [Wang_2011_IAU_273]

Wang, H., Deng, N., Liu, C.: 2012, Rapid transition of uncombed penumbrae to faculae during large flares. *Astrophys. J.* **748**, 76. DOI. [Wang_2012_ApJ_748]

Wang, H., Spirock, T.J., Qiu, J., Ji, H., Yurchyshyn, V., Moon, Y., Denker, C., Goode, P.R.: 2002, Rapid changes of magnetic fields associated with six X-class flares. *Astrophys. J. Lett.* **576**, 497. DOI. [Wang_ApJ_2002_576]

Wang, H., Liu, C., Deng, Y., Zhang, H.: 2005, Reevaluation of the magnetic structure and evolution associated with the Bastille day flare on 2000 July 14. *Astrophys. J.* **627**, 1031. DOI. [Wang_ApJ_2005_627]

Wang, S., Liu, C., Deng, N., Liu, Y., Wang, H.: 2012a, Response of the photospheric magnetic field to the X2.2 flare on February 15. *Astrophys. J. Lett.* **745**, L17. DOI. [Wang_2012_ApJL_745]

Wang, S., Liu, C., Deng, N., Wang, H.: 2014, Sudden photospheric motion and sunspot rotation associated with the X2.2 flare on 2011 February 15. *Astrophys. J. Lett.* **782**(2), L31. DOI. [Wang_2014_ApJL_782-2-L31]

Welsch, B.T., Longcope, D.W.: 2003, Magnetic helicity injection by horizontal flows in the quite Sun. I. Mutual-helicity flux. *Astrophys. J.* **588**, 620. DOI. [Welsch_ApJ_2003_588]

Yang, G., Xu, Y., Cao, W., Wang, H., Denker, C., Rimmele, T.R.: 2004, Photospheric shear flows along the magnetic neutral line of active region 10486 prior to an x10 flare. *Astrophys. J. Lett.* **617**, L151. DOI. [Yang_2004_ApJL_617]

Zhang, J., Li, L., Song, Q.: 2007, Interaction between a fast rotating sunspot and ephemeral regions as the origin of the major solar event on 2006 December 13. *Astrophys. J. Lett.* **662**, L35. DOI. [Zhang_2007_ApJL_662]